

Review

Metal Oxide Nanostructures in Food Applications: Quality Control and Packaging

Vardan Galstyan ^{1,*} , Manohar P. Bhandari ¹ , Veronica Sberveglieri ^{2,3} ,
Giorgio Sberveglieri ^{1,3} and Elisabetta Comini ^{1,3}

¹ Sensor Lab, Department of Information Engineering, University of Brescia, Via Valotti, 9, 25133 Brescia, Italy; m.bhandari@unibs.it (M.P.B.); giorgio.sberveglieri@unibs.it (G.S.); elisabetta.comini@unibs.it (E.C.)

² IBBR-CNR, Via Madonna del Piano, 10, 50019 Sesto Fiorentino, Florence, Italy; veronica.sberveglieri@ibbr.cnr.it

³ Nano Sensor Systems s.r.l., Via Branze, 38, 25123 Brescia, Italy

* Correspondence: vardan.galstyan@unibs.it

Received: 26 February 2018; Accepted: 12 April 2018; Published: 14 April 2018



Abstract: Metal oxide materials have been applied in different fields due to their excellent functional properties. Metal oxides nanostructuring, preparation with the various morphologies, and their coupling with other structures enhance the unique properties of the materials and open new perspectives for their application in the food industry. Chemical gas sensors that are based on semiconducting metal oxide materials can detect the presence of toxins and volatile organic compounds that are produced in food products due to their spoilage and hazardous processes that may take place during the food aging and transportation. Metal oxide nanomaterials can be used in food processing, packaging, and the preservation industry as well. Moreover, the metal oxide-based nanocomposite structures can provide many advantageous features to the final food packaging material, such as antimicrobial activity, enzyme immobilization, oxygen scavenging, mechanical strength, increasing the stability and the shelf life of food, and securing the food against humidity, temperature, and other physiological factors. In this paper, we review the most recent achievements on the synthesis of metal oxide-based nanostructures and their applications in food quality monitoring and active and intelligent packaging.

Keywords: metal oxide; nanostructures; gas sensor; food quality; antimicrobial activity; food packaging

1. Introduction

The monitoring and control of food quality have become important issues. The consumers and the manufacturers are paying more attention to the modern and advanced methods to check the quality of agricultural and food products and to keep them safe for a long time. Besides, the monitoring, control, and maintaining of the quality of food during its transportation from producer to consumer is another important issue. Different analytical methods for food quality control, such as the liquid chromatography–mass spectrometry [1], and surface plasmon resonance [2], have been applied. However, the aforementioned techniques have several limitations. The data acquisition and elaboration processes are slow; the instruments have relatively big dimensions and are not useful to fabricate small-size, portable systems for the real-time analysis. In this regard, the chemical sensors are very promising structures for the manufacturing of small-size and portable monitoring systems to perform real-time food quality analysis. The rotten foods produce toxin gases [3]. In addition, the metabolic activities of microorganisms in dairy foods may contribute to the breakdown of chemical compounds into volatile organic compounds (VOCs) [4]. Therefore, the detection of presence of toxins and VOCs

is necessary to avoid the hazards that are related to the food spoilage. Metal oxide based gas sensors are sensitive to a wide range of gases and VOCs. This feature makes them very attractive structures for their integration into the food quality monitoring systems [5–7]. Chemical gas sensors based on metal oxide nanomaterials have been used to evaluate and discriminate the quality and standards of all kinds of food, dairy products, and beverages [8–10]. They can be used to investigate the shelf life, freshness, and maturity of fruits, vegetables, and grains [11–13], and to assess the real-time process monitoring, including the harvesting, processing and storage [14].

The packaging technology is another important subject of research and plays a key role in food protection and storage. The active packaging involves the usage of metal oxide nanostructures in food packaging material that prolongs the shelf life, safety, and quality of the packaged product. The modern model of packaging is the intelligent packaging system with the multifunctional possibilities, such as the sensing, recording, and communication providing information about the possible problems. The spoiled food creates poison and the vapors that can be detected by the chemical gas sensors. The identification of emitted vapors from the food (milk, cheese, meat, fish, fruits, vegetables, eggs, and drinks) will be possible in order to avoid future dangers at the beginning of the spoiling process. Monitoring and control of the humidity and temperature during the food packaging and transport are important as well. Some metal oxides have a good response to the humidity changes [15–17]. This feature of oxide materials can be used for the fabrication of humidity sensors and their integration into food quality monitoring systems in order to overcome the problems that are related to the spoilage of food.

The fabrication of small-size sensing systems based on metal oxide gas sensors and their combination with the modern communications tools is a prospective way to perform qualitative and quantitative multi-component analysis of food products. These kind of systems can be activated and controlled by an operator responsible for organizing the intelligent food packaging, storage, and transport from the producer to consumer [6]. In addition, metal oxides can be used for the development of innovative food packaging materials due to their thermal stability, optical and catalytic properties, non-toxicity, and antimicrobial activities [18]. The research studies that have been published over the last years regarding the application of the metal oxide nanostructures in food quality control and packaging indicate that the interest on oxide materials and the investigation of their functional properties have appreciably increased. Figure 1 reports the number of publications with the topics “Metal oxide* AND food quality control OR food monitoring OR food packaging” since 2000 till 2018 March, retrieved from the “Web of Knowledge” database. This trend demonstrates the growing interest in the aforementioned fields.

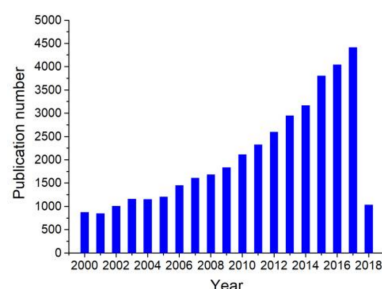


Figure 1. Number of publications with the topics “Metal oxide* AND food quality control OR food monitoring OR food packaging” since 2000, according to Web of Knowledge database.

This paper aims to provide an overview of the most recent achievements on metal oxides-based nanostructures in different food applications, including the quality monitoring, the active and intelligent food packaging, the antimicrobial activities, and the improved nutrition. We have discussed various nanofabrication technologies and strategies, showing their advantages and disadvantages.

We have highlighted the achievements and the challenges in the application of nanostructured metal oxides for the food industry.

2. Metal Oxide Nanostructures Growth and Fabrication Methods

Preparation methods of metal oxide nanostructures have been developed towards the shape, size and crystallinity control of the material. The structures can be prepared by several chemical and physical methods. These synthesis techniques of the nanomaterials are based on the top-down and bottom-up approaches. The top-down approach is advantageous in the semiconductor industry and it has been used for the fabrication of computer chips and other products. This approach is mainly based on the lithographic techniques and has limited capabilities [19]. Instead, the bottom-up approaches are in the development stage and the researchers continue to carry out experiments to improve these techniques. The schematic of top-down and bottom-up approaches is presented in Figure 2.

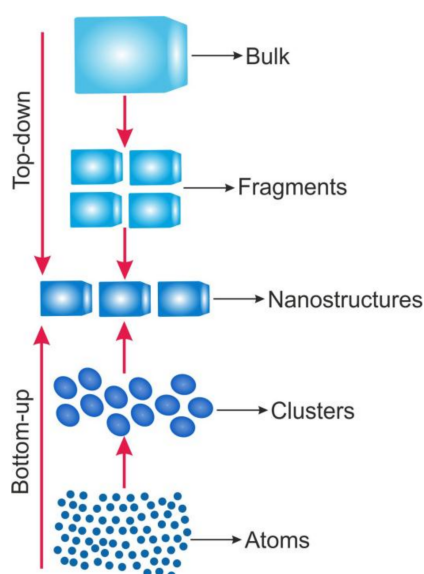


Figure 2. The schematic representation of the top-down and bottom-up approaches for the fabrication of metal oxide nanostructures.

The studies have shown that the bottom-up preparation methods may offer unique capabilities in nanofabrication. Based on this approach, the metal oxide nanostructures can be synthesized in the shape of nanowires, nanorods, nanotubes, nanobelts, etc. [5,20,21]. The assembly of molecular building blocks or chemical synthesis through the vapor phase transport, electrochemical deposition, and solution-based or template-based growth are on the basis of preparation procedures. These procedures may include the vapor-solid or vapor-liquid-solid growth, chemical or physical vapor deposition, metal organic chemical vapor deposition, and the thermal oxidation of metals [21–24]. The vapor phase deposition method is mainly performed at elevated temperatures under the gas flow in a chamber [23,25]. Great efforts have been made for the fabrication of one dimensional (1D) and thin film metal oxide nanostructures using the chemical vapor deposition (CVD) method, which involves the formation of nanomaterials onto the substrate by the chemical reactions of vapor phase precursors [5,26–28]. In this case, the reactions can be enhanced by higher frequency radiation and plasma [26,29,30]. The structure and morphology of the prepared materials depend on the substrate temperature, composition, and the chemistry of the vapor phase. Further improvements of the CVD process allowed for the fabrication of doped 1D metal oxides [26,30,31]. However, the growth rate of the nanostructure can be decreased depending on the doping concentrations [26]. Some dopants

can affect the crystal quality of the material and the material growth may become disordered due to the phase separation [30].

Atomic layer deposition (ALD) can also be used for the fabrication of 1D metal oxide materials. ALD is a modification of the CVD, in which gaseous precursors are introduced sequentially to the surface of the substrate and the reactor is purged with an inert gas to remove the unreacted precursor and the reaction byproducts [5,32]. This is a very precise template-based technique to grow well-ordered structures with uniform dimensions. The template material, its preparation and post-growth removal procedure have crucial effects on the fabrication of materials. The most used template for the ALD is the anodic aluminum oxide (AAO) [6]. Well-ordered nanotubular arrays, nanorods, nanopillars, and nanochannels were obtained using the ALD method. The diameter of the structures can be controlled by varying the pattern dimensions. Similarly, it is possible to increase the length of the obtained structures by repeating the deposition cycles [33–35].

Vapor-liquid-solid or vapor-solid growth mechanism can be involved in the physical vapor deposition (PVD) procedure for the fabrication of metal oxide nanomaterials as well. The deposition process is carried out in the furnace that is connected with a vacuum pump. The catalyst on the substrate, temperature, and pressure during the material fabrication affect the morphology of the obtained structures [5,32,36]. This is an effective method to obtain metal oxide nanowires, nanorods, nanoneedles, etc. [37,38]. The thermal oxidation of metallic layers can be used in order to obtain single crystalline metal oxide nanowires and nanorods [24,39,40]. This method may be included in the PVD category. The thermal oxidation procedure is the simplest in the PVD category and it can be carried out under atmospheric pressure. The growth conditions can be controlled by modifying the preparation procedure, the temperature, and time, as well as the metal-catalyst and gas atmosphere. Nevertheless, the fabrication procedure at high temperatures can limit the choice of the substrates, especially the use of polymeric flexible films that have relatively low-temperature stability. In this regard, the electrochemical anodization of metallic films is an effective method for the fabrication of 1D oxide materials on flexible polymeric substrates. The anodization procedure is performed in a two-electrode system electrochemical cell. This procedure consists of the oxidation and etching of the metallic films. The metals can be anodized in normal ambient conditions at room temperature [22]. Well-ordered and highly aligned tubular arrays and porous structures can be obtained by means of the anodization method. The length and diameter of the structures are controlled by a variation of the electrolyte composition, the reaction time, and the anodization voltage [41–43]. The synthesis procedure at relatively low temperatures allows for fabricating the nanomaterials on flexible polymeric substrates [44,45]. More complex architectures (Figure 3) can be obtained by coupling the electrochemical anodization and the thermal decomposition methods [45].

Chemical methods, such as the spin-coating, dip-coating, and sol-gel have been applied for the preparation of metal oxide thin films and nanoparticles [46–48]. The aforementioned methods are very convenient for the fabrication of composite structures due to the availability of precursor materials [47–49]. The morphology, alignment, density, aspect ratio, and crystalline quality of the materials that were prepared by sol-gel are directly related to the seed layer parameters [46]. Recent investigations have shown that the hydrothermal growth using different chemical solutions is another efficient method for the preparation of pure and doped oxide materials with various shapes (nanorods, nanofibers, nanowires, and nanosheets) [50–53]. The morphology of the structures during the preparation process is changed depending on the solution composition, the reaction temperature, and time [6,54].

To prepare the hierarchically assembled poly- and single-crystalline 1D metal oxide nanostructures, the ALD, PVD, CVD, and thermal oxidation methods have been well developed comparing to the chemical approaches. Meanwhile, the template-assisted approach, such as the ALD, makes the integration of the material difficult with the existing planar structures. The growth rate and the crystallinity of the nanostructures that are prepared through the vapor phase transport can be reduced depending on the dopant material type and concentration. The anodization is a cost-effective

and precise method to obtain well-ordered and doped nanotubes or nanoporous structures at room temperature without the use of any vacuum technique. Nevertheless, the anodized materials are mainly amorphous and they can be crystallized by post-growth thermal treatment. The doping and functionalization of metal oxides with the different materials can be successfully performed by means of the hydrothermal growth. In this case, the structure synthesis is performed at high temperatures, which limits the choice of substrates.

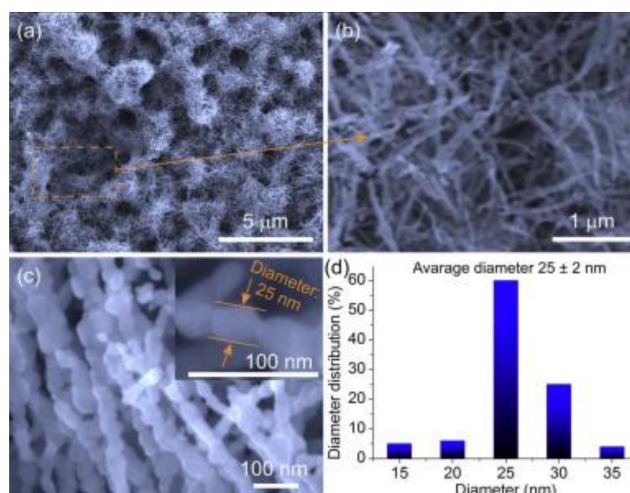


Figure 3. (a–c) SEM micrographs with different resolutions and (d) corresponding histograms of thermally annealed ZnO nanoparticles diameter distribution. Reprinted from [45] with permission. Copyright (2015) Elsevier B.V.

3. Food Quality Control

This section reports the recent developments in metal oxide chemical sensor devices for their applications in food analysis, in particular, the food quality control, process monitoring, authenticity, and freshness determination. The sensing mechanism of metal oxides is related to the adsorption and desorption processes of different gaseous compounds on the structure surface, followed by the changes in the material electrical conductance (or resistance). The sensing mechanism is described in more detail in our previous works [5,6]. Recent studies have shown that the metal oxide nanomaterials-based gas sensors can be used for the assessment of food products. Chemical sensors and more complex systems have been used to detect the gases that are present in the rotten or spoiled food.

Trimethylamine (TMA) is a gaseous compound that is formed naturally due to the biodegradation of fish and animal products. TMA detection may give useful information to determine the fish and the seafood freshness. TiO_2 , WO_3 , and ZnO with different shapes showed a good response towards TMA [55–58]. The functionalization of WO_3 nanorods, ZnO (Figure 4) and MoO_3 by Au improved the material's response due to the catalytic effect of Au [56,58,59]. Introduction of Cr^{3+} in 1D ZnO nanostructures or their coupling with Cr_2O_3 and In_2O_3 can enhance the response and selectivity of the materials towards TMA [57,60,61]. In addition, the heterostructure based on p-type Cr_2O_3 and SnO_2 nanowires showed a good and selective response towards low concentrations of TMA [62]. Lou et al. fabricated the $\alpha\text{-Fe}_2\text{O}_3/\text{TiO}_2$ hierarchical heterostructure with a good sensing performance when compared with the pure Fe_2O_3 and TiO_2 1D nanostructures [63]. Dimethylamine (DMA) and ammonia (NH_3) are the other substances that are responsible for fishy odors, and directly related to the fish quality [64]. During the last years, only a couple of works have been published on metal oxide-based DMA sensors. Investigations have shown that 1D ZnO materials have very good sensing properties for the fabrication of DMA gas sensors [65,66]. However, there is no detailed information in the literature on the studies of other metal oxide materials for their application in DMA detection. Hence, the perspectives of the application of other oxide materials in the fabrication

of DMA sensors are still not clear. Besides the fish quality control, NH_3 was used as an analyte to determine the shelf life and spoilage of other meat products [67]. The sensing performance of oxide materials towards NH_3 was improved by combining them with polymers. SnO_2 nanosheets and ZnO nanorods were polymerized by the polypyrrole [68,69]. The response of the polypyrrole- SnO_2 composite towards a low concentration of NH_3 was improved because of the p-n junction that was formed at the interface of two materials [68]. Excellent conjunction and interaction between the polypyrrole chains and the ZnO nanorods improved the charge transfer in the composite enhancing the structure response [69]. Moreover, both of the composite materials showed a selective response towards NH_3 at room temperature (RT), which is an important achievement to fabricate low power consumption sensing devices. The coupling of TiO_2 and ZnO with the polyaniline also improved the response and selectivity of the materials at RT [70,71]. The functionalization of ZnO nanorods by Au enhanced the sensing performance of the structure at RT, and in the meantime, decreased the response and recovery time of ZnO [72]. Li et al. improved the response of SnO_2 nanotubes towards NH_3 at RT by fabricating a $\text{SnO}_2/\text{SnS}_2$ composite material [73]. This improvement was attributed to the heterojunction that was formed at the boundaries of SnO_2 and SnS_2 crystallites and the higher work function of SnS_2 as compared with SnO_2 .

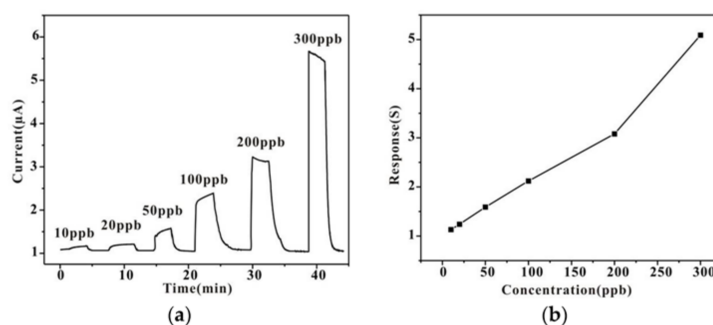


Figure 4. (a) Responses of the Au-modified hierarchical porous single-crystalline ZnO nanosheets to different concentrations of trimethylamine (TMA) and (b) the corresponding calibration curve. Reprinted from [58] with permission.

Hydrogen sulfide (H_2S) is produced from eggs and egg products due to their heating. Moreover, low concentrations of H_2S contribute to the flavor of heated proteinaceous foods, such as beef, chicken, fish, and milk products, and its production increases at higher temperatures. The detection of H_2S can give useful information to identify the overcooked and rotten food [74]. Various oxide materials and their compositions have been studied for the fabrication of H_2S sensors [75–84]. Porous metal oxide nanostructures, such as TiO_2 , NiO, and CuO are very attractive materials for H_2S detection [75–77,85]. They have shown a good response towards low concentrations of H_2S . In addition, the porous NiO and CuO with p-type conductivity could detect H_2S in ppb level at relatively low operating temperatures [76,77]. TiO_2 nanoparticles have been used for the functionalization of Fe_2O_3 nanorods [83]. The obtained structure showed a better sensing performance when compared to the pristine Fe_2O_3 nanorods. The enhancement was related to the modulation conduction channel width and potential barrier height of the material. The functionalization and doping of ZnO have been proven as the promising strategies to improve the material response towards H_2S [86,87]. Guo et al. fabricated a composite material based on ZnO and SnO_2 [80]. The obtained ZnO/ SnO_2 heterogeneous nanospheres showed selective and high response in the presence of low concentrations of H_2S . Ag-loaded yolk-shell SnO_2 nanostructures showed a high and reversible response towards H_2S [81]. Yang et al. reported the synthesis of $\text{Ag}_2\text{O}/\text{SnO}_2$ porous structures with the stable and selective response towards H_2S in ppb level [82]. The H_2S sensing performance of a p-n junction based on $\text{Co}_3\text{O}_4\text{-SnO}_2$ nanocomposite was improved with an increase in the structure annealing temperature [79]. CuO/ V_2O_5 hybrid nanowires showed a better response towards H_2S when compared with the pristine V_2O_5 nanowires [78].

Fruits and vegetables are perishable products with a very short shelf life. The detection of VOCs is an accessible way for the monitoring of changes in the fresh produce. The majority of the latest studies have been carried out to develop metal oxide sensors for the detection of ethanol and acetone. SnO₂, ZnO, TiO₂, Cr₂O₃, WO₃, Co₃O₄, NiO, and In₂O₃ based nanostructures with different morphologies have been studied for the ethanol [4,88–92] and acetone detection. Reported results have shown that the functionalization and introduction of specific dopant materials can improve the response, selectivity, and recovery time of oxide materials. Furthermore, the composite structures based on metal oxides have shown a promising sensing performance for their application in ethanol and acetone sensing devices. Table 1 summarizes the recent achievements in sensing properties of the metal oxide-based structures for the food quality analysis.

Table 1. A selected list of references on metal oxide materials for the fabrication of gas sensors and their application in food quality analysis.

| Material and Morphology | Target Gas and Concentration | Operating Temperature (°C) | Reference |
|--|---------------------------------|----------------------------|-----------|
| TiO ₂ nanotubes | TMA, 40–400 ppm | - | [55] |
| Au-WO ₃ nanorods | TMA, 100 ppm | 280 | [56] |
| Au-MoO ₃ nanobelts | TMA, 5–100 ppm | 280 | [59] |
| Cr ³⁺ -ZnO nanorod | TMA, 0.01–100 ppm | 255 | [57] |
| ZnO-Cr ₂ O ₃ | TMA, 5 ppm | 400 | [60] |
| ZnO-In ₂ O ₃ nanofibers | TMA, 0.05–5 ppm | 375 | [61] |
| Cr ₂ O ₃ -SnO ₂ nanowire | TMA, 0.25–5 ppm | 450 | [62] |
| Au-ZnO porous nanosheets | TMA, 10–300 ppm | 260 | [58] |
| α-Fe ₂ O ₃ /TiO ₂ nanofibers/nanorods | TMA, 10–200 ppm | 250–320 | [63] |
| ZnO pencil-like | DMA, 5–300 ppm | 340 | [65] |
| ZnO nanorod/nanosheet | DMA, 1–1000 ppm | 370 | [66] |
| polypyrrole-SnO ₂ nanosheets | NH ₃ , 1–10.7 ppm | RT | [68] |
| polypyrrole-ZnO nanorods | NH ₃ , 50 ppm | RT | [69] |
| Polyaniline-TiO ₂ thin films | NH ₃ , 23–141 ppm | RT | [70] |
| Polyaniline-ZnO nanoparticles | NH ₃ , 20–100 ppm | RT | [71] |
| Au-ZnO nanorods | NH ₃ , 5–100 ppm | RT | [72] |
| SnO ₂ /SnS ₂ nanotubes/nanoparticles | NH ₃ , 20–500 ppm | RT | [73] |
| TiO ₂ nanotubes | H ₂ S, 1–50 ppm | 300 | [85] |
| TiO ₂ nanotubes | H ₂ S, 6–38 ppm | 70 | [75] |
| NiO porous | H ₂ S, 1 ppb–100 ppm | RT–92 | [76] |
| CuO porous nanosheets | H ₂ S, 10 ppb–60 ppm | RT | [77] |
| TiO ₂ -Fe ₂ O ₃ nanoparticle-nanorods | H ₂ S, 1–200 ppm | 300 | [83] |
| Au-ZnO nanorods | H ₂ S, 3 ppm | 25 | [86] |
| Cu-ZnO thin film | H ₂ S, 5–50 ppm | 250 | [87] |
| ZnO/SnO ₂ , nanospheres | H ₂ S, 0.5–100 ppm | 300 | [80] |
| Ag-SnO ₂ , yolk-shell | H ₂ S, 0.25–5 ppm | 350 | [81] |
| Ag ₂ O/SnO ₂ porous | H ₂ S, 300 ppb | 100 | [82] |
| Co ₃ O ₄ -SnO ₂ nanobox | H ₂ S, 50 ppm | 180 | [79] |
| CuO/V ₂ O ₅ nanowires | H ₂ S, 7–23 ppm | 220 | [78] |
| PbO-SnO ₂ nanowires | Ethanol, 5–200 ppm | 300 | [88] |
| Reduced graphene oxide-ZnO, nanoparticles, chain-like agglomerates | Ethanol, 100–250 ppm | 250 | [4] |
| TiO ₂ nanotubes | Ethanol, 10–50 ppm | 200–500 | [89] |
| Cr ₂ O ₃ -WO ₃ , nanoparticle, nanorods | Ethanol, 5–200 ppm | 300 | [90] |
| Co ₃ O ₄ porous nanosheets | Ethanol, 1–100 ppm | 220 | [91] |
| Cd-NiO thin film | Ethanol, 1000 ppm | 100 | [92] |
| PtO ₂ -SnO ₂ nanofiber | Acetone, 0.6–5 ppm | 400 | [93] |
| Fe-C-WO ₃ walnut-like particles | Acetone, 0.2–10 ppm | 300 | [94] |
| W-NiO, flower-like spheres | Acetone, 10–1000 ppm | 250 | [95] |
| In ₂ O ₃ -reduced graphene oxide, nanocubes | Acetone, 5–25 ppm | 175 | [96] |

The presence of VOCs in food is a complex aroma bouquet, which includes different compounds due to the aging and bacterial putrefaction of food. In this regard, the fabrication of a more complex and multicomponent system is a proper way for the precise monitoring of food quality and discrimination. The concept of this artificial system is called Electronic nose (EN). An EN consists of different metal oxide gas sensors, where each sensor has particular application requirements with a specific response and selectivity to recognize simple or complex gaseous compounds.

Konduru et al. used SnO₂ and WO₃ based sensors array to differentiate ethanol, acetone, acetonitrile, and ethyl acetate for the onion quality evaluation. The fabricated EN sensing system was able to detect the presence of the two key volatile compounds that were emitted by diseased onions, and in the meantime, to differentiate them at two concentration levels [97]. An EN based on SnO₂ chemical sensors was applied for the identification of the geographical origin of licorice roots [98]. E-nose results were compared to the results that were obtained by the other techniques. The investigations showed that this is an effective and non-destructive method for the authentication of licorice roots. Pacioni et al. used SnO₂ sensors array that was functionalized with different metals to obtain a good and selective response towards acetaldehyde, ethanol, acetone, dimethylsulfide, and ethylacetate for the discrimination of truffle-flavored oils [99]. The SnO₂ is the most studied metal oxide material for the fabrication of gas sensors. The material has a good response towards different gases. Therefore, the SnO₂ based chemical sensors have been mostly used for the fabrication of EN systems. The ENs based on SnO₂ gas sensors have been applied for the classification of black tea and the diagnosis of Enterobacteriaceae in vegetable soups, to study the global aromatic profile of coffee, as well as for the meat and fish freshness control. The applications of EN systems based on SnO₂ and the other metal oxides are summarized in Table 2. Unfortunately, the composition of oxide materials in some studies on EN systems was not presented. This fact makes it difficult to perform a more detailed comparison of the results that were reported in the literature.

The recent studies of oxide materials are mainly focused on the nanostructures and the thin films, with an increasing attention to improve the sensing performance of the material at relatively low operating temperatures for the prototype sensing devices [100–102]. Furthermore, the water molecules can be formed on the surface of metal oxides due to the adsorption of some reducing gases [103]. Therefore, to obtain the gas sensors with stable and reversible response, the sensor device should operate above room temperature to avoid the effects that are related with the water molecules. The aforementioned issues should be considered when comparing the operating temperature and the power consumption of the sensing devices. The different sensing behaviors that were reported for the doped and functionalized oxide materials towards different gaseous compounds are encouraging, and together with the use of ENs, will reduce the problem of the selectivity. The accurate control of the structures shape, composition and dimensions will contribute towards the synthesis of new and interesting nanomaterials, which will open unexplored possibilities for future sensing technologies for food quality control applications.

Table 2. A list of Electronic nose (EN) systems based on metal oxides for the food quality monitoring.

| Sensing Material | Target Gases | Application | Reference |
|---|--|---|-----------|
| SnO ₂ , WO ₃ | Ethanol, acetone, acetonitrile, ethyl acetate | Onion quality evaluation | [97] |
| SnO ₂ | Ethanol, ethyl acetate, isobutyl alcohol, etc. | To identify geographical origin of Licorice roots | [98] |
| SnO ₂ , SnO ₂ -SiO ₂ , Ag-SnO ₂ , Au-SnO ₂ , Pd-SnO ₂ , WO ₃ | Acetaldehyde, ethanol, acetone, etc. | To distinguish truffle-flavored oils | [99] |

Table 2. Cont.

| Sensing Material | Target Gases | Application | Reference |
|--|---|--|-----------|
| SnO ₂ | Aromatic compounds | Classification of Indonesian black tea | [104] |
| SnO ₂ | Alcohols, aldehydes, ketones, etc. | To study the global aromatic profile of coffee | [105] |
| SnO ₂ , MoO ₃ | Acids, alcohols | Diagnosis of Enterobacteriaceae in vegetable soups | [106] |
| SnO ₂ | Aromatic compounds | To study the quality of tea | [107] |
| Metal oxide sensors, Hanwei Electronics Co., Ltd. | Alcohols, NH ₃ | Prediction of banana quality | [108] |
| Metal oxide sensors, Hanwei Electronics Co., Ltd. and Figaro Inc. | Sulfur compounds, H ₂ S, NH ₃ | Classification of garlic cultivars | [109] |
| Metal oxide sensors, PEN2, Airsense Analytics, Germany | Alcohol, NH ₃ , aromatic compounds | Strawberry juice quality control | [110] |
| Metal oxide sensors, Figaro USA Inc. | VOCs | Fish species discrimination | [111] |
| Metal oxide sensors, Alpha M.O.S., France | Organic acids, caffeine | Aromatic profile of Espresso coffee | [112] |
| Metal oxide sensors, Ogam Technology, Futurlec, e2v and Figaro Engineering | VOCs, NH ₃ , alcohol, etc. | Meat and fish freshness control | [113] |
| Metal oxide sensors, Alpha M.O.S., France | Ethanol, NH ₃ , VOCs | To trace peanuts quality | [114] |
| Metal oxide sensors, Win Muster Airsense Analytics Inc., Germany | Alcohol, methane, aromatic compounds | Analysis of edible oil oxidation | [115] |
| Metal oxide sensors, Hangzhou Ke Na Sensors Inc., and Figaro Inc. | TMA, DMA, Ethanol | Freshness control of hairtail fish and pork | [116] |
| Metal oxide sensors, Figaro Inc., Japan | Ethanol, NH ₃ , VOCs | Classification of honey | [117] |

4. Food Packaging and Antimicrobial Actions

In this section, the most active metal oxide nanostructures that have been exploited for use in the food packaging systems are reviewed, along with their structure, effects, and applications.

TiO₂ nanoparticles are good photocatalysts and antimicrobial agents that are used in food packaging [118–121]. They act upon the food spoilage bacteria through lipid peroxidation that is caused by the production of reactive oxygen species (ROS) molecules under visible and UV, DNA damage via hydroxyl radicals, resulting in cell death [122,123]. TiO₂ based bio-nanocomposites have been used as the efficient packaging materials for various oxygen-sensitive food products [124]. An interesting work on TiO₂ based bio-nanocomposite film as a packaging material for soft white cheese was presented by Youssef et al. [125]. The material consisting of chitosan, poly (vinyl alcohol), and TiO₂ nanoparticles (CS/PVA/TiO₂) exhibited good mechanical properties and antimicrobial activities against Gram-positive, Gram-negative bacteria, fungi, and coliform. In another study, they used ZnO nanoparticles, chitosan (CH), and carboxymethyl cellulose (CMC), namely CH/CMC/ZnO nanocomposite, as a packaging material for the same cheese [126]. It showed similar properties as the TiO₂-based material. The CS/PVA/TiO₂ bio-nanocomposites displayed hydrophobic property and when used as a packaging material for the soft white cheese, the moisture content of the cheese

significantly increased with increasing storage period. In case of CH/CMC/ZnO packaged cheese, the textural parameters of the cheese reduced with the storage time and few changes were also reported as compared to the control and blank. The films had a significant impact on pathogenic microbial strains presented with the inhibition zone ranging from 5 to 15 mm. A poly(vinyl-chloride) PVC/TiO₂ nanocomposite bears an efficient food packaging property, mechanical strength, and antimicrobial properties [127]. He et al. prepared a TiO₂-protein/polysaccharide (marine red alga) nanocomposite film, wherein the TiO₂ nanoparticles enhanced the tensile strength of the film, showed an antimicrobial action against the food pathogen bacteria *E. coli* and *S. aureus*, and maintained the quality and shelf life of cherry tomatoes when being used as a coating material [128]. By increasing the TiO₂ content in starch/TiO₂ bio-nanocomposite, the hydrophobicity of the nanocomposite increased, and its thermal, mechanical, and UV light-shielding properties were enhanced [129].

The nano-TiO₂-low density polyethylene (LDPE) packaging showed promising results in maintaining the quality and shelf life of Pacific white shrimp [130]. The TiO₂-LDPE nanocomposite material inhibited the growth of spoilage bacteria and lowered the polyphenol oxidase (PPO) activity. It was able to retard the decrease of whiteness and water holding capacity, and reduced the total viable counts (TVC). Bodaghi et al. demonstrated the ability of TiO₂-LDPE nanocomposite film to inhibit the microorganisms *Pseudomonas* spp. and *Rhodotorula mucilaginosa* that are responsible for fruit and vegetable spoilage [131]. The same group developed an LDPE/clay-TiO₂ nanocomposite film showing strong mechanical and barrier properties, and convincing antimicrobial activities against the aforementioned classes of microorganisms [132]. Such film is useful in horticulture product packaging. Similarly, mesoporous TiO₂/SiO₂ nanocomposite with different concentrations of nanoparticles was used to degrade ethylene under UV light as a measure to ensure the shelf life of mature green tomatoes. This could be a successful photooxidative packaging film model for the fresh fruits and vegetables, and their postharvest management [133]. Chitosan/TiO₂ nanocomposite film also demonstrated ethylene photodegradation that helped in the prolongation of tomato storage [134]. TiO₂ nanoparticles were exploited to construct a biodegradable nanocomposite film that was aimed at preserving the microbial and sensory qualities of lamb meat during storage [135]. The whey protein isolate (WPI)/cellulose nanofiber (CNF)/TiO₂ nanoparticles/rosemary essential oil (REO) nanocomposite film was successful in reducing the bacterial load containing food pathogens, such as *L. monocytogenes*, *S. enteritidis*, *E. coli* O₁₅₇:H₇, *S. aureus*, and *P. fluorescens*, thus increased the shelf life of the meat. Another biodegradable nanocomposite film that was fabricated by incorporating jackfruit filum polysaccharide (JFPS)-TiO₂ nanoparticles displayed reduced moisture content, transparency, and total soluble matter [136]. The JFPS/TiO₂ nanocomposite showed an excellent antimicrobial action that was essential for active food packaging.

In view of the food preservation and safety, various methods and composite materials have been employed for the long-term food storage. AgCl-TiO₂ nanocomposite material was used to study the anti-quorum sensing mechanism [137]. Quorum sensing system has been linked to the biofilm formation in food spoilage bacteria. In this study, the anti-quorum sensing activity of the bioactive AgCl-TiO₂ material in the model bacteria *Chromobacterium violaceum* was confirmed by the absence of signaling molecule oxo-octanoyl homoserine lactone during bacterial growth, endorsing the potential use of AgCl-TiO₂ nanomaterial in the food packaging industry. Peter et al. developed Ag/TiO₂-SiO₂-coated food packaging film for the preservation of fresh green lettuce during storage [138]. The obtained results showed its ability to reduce the level of lettuce spoilage, known as botrytis blight that is caused by *Botrytis cinerea*. The antimicrobial action of TiO₂ nanomaterial is explained by its capacity to produce charge carriers when exposed to UV light, which initiates redox reaction on the microbial cell surface that eventually inhibits the microbial cell. Ag/TiO₂ nanocomposite-based packaging extended the shelf life and microbial safety of the white bread by inhibiting the growth of yeast, molds and Gram-positive bacteria *B. cereus* and *B. subtilis* [139]. In another study, the microbiological and chemical characteristics of the white bread during storage in paper packages using Ag/TiO₂-SiO₂, Ag/N-TiO₂, or Au/TiO₂ in comparison with the non-modified

paper packages were investigated [140]. The tensile and breaking resistance of the paper packages decreased with an increase in the composite content. The Ag/TiO₂-SiO₂ based-paper showed the best properties; all three of them exhibited superior water retention and the nanocomposites containing Ag nanoparticles extended the shelf life of the bread together with a strong antimicrobial action.

Poly lactic acid (PLA) nanocomposite films prepared from TiO₂ and Ag nanoparticles were applied to study their antimicrobial properties and shelf life of Yunnan cottage cheese [141]. The obtained results showed the essential antimicrobial properties of the PLA/TiO₂ and PLA/TiO₂+Ag packaging films and the packed cheese exhibited better retention in pH value, lactic acid bacteria (LAB) count, and sensory quality. TiO₂-potato starch blend films were studied where TiO₂ nanoparticles reduced the water solubility, water vapor permeability, and moisture uptake of the film [142]. The overall functional properties of the film were improved, illustrating its potential for food packaging. Likewise, a soluble soybean polysaccharide (SSPS)/TiO₂ bio-nanocomposite showed excellent heat seal strength and biocidal activities fulfilling the requisites for a food coating and packaging material [143]. Other TiO₂-based nanocomposite films that were applicable in active and intelligent food packaging are: fish bilayer gelatin/agar film containing TiO₂ [144], wheat gluten/cellulose nanocrystals/TiO₂ nanocomposite [145], and TiO₂/LDPE film assuring the food safety and quality [146]. A chitosan-TiO₂ nanocomposite that was prepared for packaging red grapes was successful in preventing the microbial infection and elongating the shelf life of the grapes [147]. It should be noted that the nanocomposites showed better mechanical properties and enhanced hydrophilicity or high-water permeability. It was efficient against both Gram-positive and Gram-negative bacteria by provoking the leakage of cellular substances through the damaged membrane. Similarly, TiO₂ and Ag-doped TiO₂ nanoparticles were reported to show photocatalytic antibacterial performance under visible-light irradiation [148]. The viability of the test microorganisms: Gram-positive *S. aureus* and Gram-negative *P. aeruginosa*, *E. coli* bacteria was reduced to zero at 3% and 7% doping concentrations of Ag-TiO₂ nanoparticles. TiO₂ offers a good supporting material for the doping of Ag nanoparticles due to its small size and high surface area. A novel bio-nanocomposite material that was developed from wheat gluten, nanocellulose, and TiO₂ nanoparticles coated in kraft paper sheets for food packaging applications showed good antibacterial properties against Gram-positive and Gram-negative bacteria expressed in terms of reduction% of surviving number (CFU) of the tested organisms [145]. A simple example of active food packaging procedure exploiting the polymer nanocomposites is shown in Figure 5.

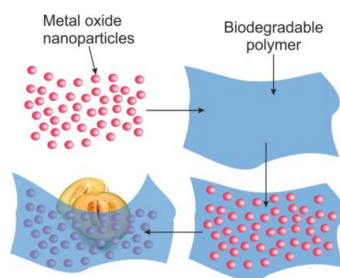


Figure 5. Schematic representation of the active food packaging using metal oxide nanostructure and biodegradable polymeric films.

ZnO nanoparticles are effective antimicrobial agents when they are present in reduced particle size and dimension. They demonstrate an excellent antimicrobial activity against the food pathogens, like *Salmonella*, *Klebsiella*, and *Shigella* via the generation of ROS and the loss of membrane integrity. ZnO nanoparticles also exhibit antibacterial action against spores that are high temperature and pressure resistant [149]. Among the ZnO/LDPE, TiO₂/LDPE, and ZnO-TiO₂/LDPE nanocomposite films that were studied against *E. coli* in fresh calf minced meat, ZnO/LDPE films were identified as the best materials to prevent bacterial growth and to improve the shelf life of the meat [150]. An active emulsified film that was based on carboxymethyl cellulose-chitosan-oleic acid (CMC-CH-OL) with

ZnO nanoparticles that were produced by the casting method was found to be active against the fungi *Aspergillus niger*, and its extensibility increased [151]. The nanocomposite film was effectively applied to increase the shelf life of sliced white bread [152]. All active coatings reduced the number of yeasts and molds in the bread. An active polymer bilayer polyethylene/polycaprolactone (PE/PCL) film that was modified with ZnO or ZnO/casein complex extended the shelf life of food [153]. The addition of ZnO nanoparticles enhanced the barrier, mechanical, thermal properties, and antimicrobial actions of the nanocomposite film. This helps in protecting the food products during their transport. Therefore, such a nanocomposite material is preferred for food packaging when low water loss from packaging is favorable. The use of polyethylene films with chitosan-ZnO nanocomposite for active food packaging prevented the microbial contamination after 24 h incubation and extended the shelf life of food [154]. ZnO nanoparticles that were introduced into the chitosan matrix showed a 42% increase in solubility (water affinity) and an 80% reduction in swelling of the resultant nanocomposite materials. The mechanical, thermal, and antimicrobial effect of TiO₂ and ZnO added PET-poly(ethylene terephthalate) and PBS-poly(butylene succinate) blend thin film was shown by Threepopnatkul et al. [155]. The PET/PBS thin film with TiO₂ seemed to be effective against *E. coli* and *S. aureus* than that with ZnO, showcasing the use of the material for food packaging applications.

A comprehensive list of metal oxide nanomaterials and nanocomposites in active food packaging and analysis is given in Table 3. Since the advent of innovative metal oxide nanostructured materials in food packaging, this field continues to grow and evolve. Whereas, these metal oxide nanocomposites serve as a boon in active and intelligent packaging research. There have been concerns about the safety, sustainability, and potential health risks and hazards of the materials that were used. The nanomaterials, when utilized as food additives, could transfer to the food matrix from the nanocomposite. Given the alterations in the nanomaterial surface and properties due to the chemical and physical transformations, the determination of such nanomaterials in a complex food matrix still poses a challenge. Hence, the important concerns that are related to the application of nanocomposites in food packaging are about the size, quantity, and physiochemical properties of the nanomaterials than the polymers, enzymes, or antimicrobial agents that are used to synthesize the nanocomposites. This provides a room for the improvement in key properties and functionalities of the nanomaterials for the food packaging applications.

Table 3. Applications of metal oxide-based nanomaterials in food packaging sector.

| Material | Application/ Mode of Action | Reference |
|--|--|-----------|
| CS/PVA/TiO ₂ | Food packaging | [125] |
| CH/CMC/ZnO | Food packaging | [126] |
| PVC/TiO ₂ | Food packaging | [127] |
| TiO ₂ -protein/polysaccharide (marine red alga) | Quality and shelf life of cherry tomatoes | [128] |
| Starch/TiO ₂ | UV-protective food packaging material | [129] |
| TiO ₂ -LDPE | Quality and shelf-life of Pacific white shrimp | [130] |
| TiO ₂ -LDPE | Antimicrobial actions in fruit and vegetable | [131] |
| LDPE/clay-TiO ₂ | Antimicrobial action, horticulture packaging | [132] |
| TiO ₂ /SiO ₂ | Degrade ethylene, quality and shelf life of mature green tomatoes | [133] |
| Chitosan/TiO ₂ | Ethylene photodegradation, prolongation of tomato storage | [134] |
| WPI/CNF/TiO ₂ /REO | Microbial and sensory qualities of lamb meat, antimicrobial action | [135] |
| JFPS-TiO ₂ | Antimicrobial action, active food packaging | [136] |

Table 3. Cont.

| Material | Application/ Mode of Action | Reference |
|--|---|-----------|
| AgCl-TiO ₂ | Anti-quorum sensing, food packaging | [137] |
| Ag/TiO ₂ -SiO ₂ | Preservation of fresh green lettuce, reduction of lettuce spoilage, antimicrobial action | [138] |
| Ag/TiO ₂ | Shelf life and microbial safety of white bread, inhibition of yeast, mold and Gram-positive bacteria | [139] |
| Ag/TiO ₂ -SiO ₂ , Ag/N-TiO ₂ or Au/TiO ₂ | Shelf life of white bread, antimicrobial action | [140] |
| PLA/TiO ₂ and PLA/TiO ₂ +Ag | Shelf-life of Yunnan cottage cheese | [141] |
| Starch/TiO ₂ | Reduced water solubility, water vapor permeability and moisture uptake of the film, food packaging function | [142] |
| Soybean polysaccharide/TiO ₂ | Heat seal strength, antimicrobial action, food coating and packaging | [143] |
| Fish gelatin/agar bilayer/TiO ₂ | Food packaging, food safety | [144] |
| Wheat gluten/CNC/TiO ₂ | Food packaging, food safety | [145] |
| TiO ₂ /LDPE | Food packaging, food safety | [146] |
| ZnO/LDPE, TiO ₂ /LDPE, and ZnO-TiO ₂ /LDPE | Antimicrobial property against <i>E. coli</i> in fresh calf minced meat, shelf life of calf meat | [150] |
| Carboxymethyl cellulose-chitosan-oleic acid/ZnO | Antimicrobial action against the fungi <i>Aspergillus niger</i> , increased extensibility | [151] |
| CMC-CH-OL-ZnO | Shelf life of sliced white bread, active against yeast and molds | [152] |
| polyethylene/polycaprolactone-ZnO | Shelf life of food, antimicrobial actions, food packaging and transport | [153] |
| Chitosan-TiO ₂ | Food packaging, effective packaging of red grapes, shelf life of grapes | [147] |
| TiO ₂ and Ag-TiO ₂ | Photocatalytic antibacterial performance, food packaging | [148] |
| Chitosan-ZnO/polyethylene | Food packaging, antimicrobial properties, shelf life of food | [154] |
| Wheat gluten/nanocellulose/TiO ₂ coated in craft paper | Food packaging, antimicrobial action | [145] |
| TiO ₂ , ZnO-poly(ethyleneterephthalate) and poly(butylene succinate) | Food packaging | [155] |

5. Conclusions

In summary, we provide a comprehensive review of recent research activities on the synthesis and application of metal oxide materials in food quality control and active and intelligent packaging. During the last years, the major part of research on the fabrication of metal oxide nanomaterials has been devoted to the improvement of the synthesis procedures for the modification of the shape and size of the structure and the incorporation of dopant or mixture materials onto the obtained structures. Investigations suggest that the move to the nanoscale can significantly increase the response of the material. The doping and fabrication of composite structures is favorable to improve the selectivity of the material. Numerous studies have showed that the gas sensors that are based on metal oxides nanomaterials are very attractive structures. This is due to their promising gas sensing properties caused by their low dimensionality and high surface-to-volume ratio. However, the advantages

and disadvantages in the fabrication methods of metal oxide nanostructures should be considered, estimating the preparation speed, cost, and reproducibility.

The EN systems can be used for the selective detection of VOCs and other gaseous compounds, which is very important for the precious determination of quality changes in the food products. ZnO, TiO₂, NiO, Cr₂O₃, WO₃, CuO, Fe₂O₃, Co₃O₄, V₂O₅, and In₂O₃ nanostructures have shown attractive sensing performances for the fabrication of chemical sensors and their applications in food quality control systems. Moreover, SnO₂ has been widely and successfully used in EN systems for the food quality analysis.

The recent studies on metal oxide nanocomposites-based food packaging emphasize the essential role of metal oxide nanomaterials in the fabrication of nanocomposite films coupling the polymer matrices, such as PE, PVC, PLA, chitosan, cellulose, and starch. The obtained bio-nanocomposite structures exhibit antimicrobial actions and effective mechanical, thermal, and barrier properties. Their application in active and intelligent food packaging ensures the food quality and safety and an increased shelf-life of food products.

Acknowledgments: The authors are thankful to Craig Evans from the Department of Information Engineering (University of Brescia) for revision of English.

Author Contributions: The authors contributed equally to this work.

Conflicts of Interest: The authors declare no conflict of interest.

References

1. Di Stefano, V.; Avellone, G.; Bongiorno, D.; Cunsolo, V.; Muccilli, V.; Sforza, S.; Dossena, A.; Drahos, L.; Vékey, K. Applications of liquid chromatography–mass spectrometry for food analysis. *J. Chromatogr. A* **2012**, *1259*, 74–85. [[CrossRef](#)] [[PubMed](#)]
2. Vežočník, V.; Hodník, V.; Anderluh, G. Surface plasmon resonance analysis of food toxins and toxicants. In *Analysis of Food Toxins and Toxicants*; John Wiley & Sons, Ltd: Hoboken, NJ, USA, 2017; pp. 195–216.
3. McCarthy, M.J.; McCarthy, K.L. *Advanced Sensors, Quality Attributes, and Modeling in Food Process Control*; Springer: Boston, MA, USA, 2013; pp. 499–517.
4. Galstyan, V.; Comini, E.; Kholmanov, I.; Ponzoni, A.; Sberveglieri, V.; Poli, N.; Faglia, G.; Sberveglieri, G. A composite structure based on reduced graphene oxide and metal oxide nanomaterials for chemical sensors. *Beilstein J. Nanotechnol.* **2016**, *7*, 1421–1427. [[CrossRef](#)] [[PubMed](#)]
5. Galstyan, V.; Comini, E.; Ponzoni, A.; Sberveglieri, V.; Sberveglieri, G. ZnO quasi-1D nanostructures: Synthesis, modeling, and properties for applications in conductometric chemical sensors. *Chemosensors* **2016**, *4*, 6. [[CrossRef](#)]
6. Galstyan, V. Porous TiO₂-based gas sensors for cyber chemical systems to provide security and medical diagnosis. *Sensors* **2017**, *17*, 2947. [[CrossRef](#)] [[PubMed](#)]
7. Moseley, P.T. Progress in the development of semiconducting metal oxide gas sensors: A review. *Meas. Sci. Technol.* **2017**, *28*, 082001. [[CrossRef](#)]
8. Baldwin, E.A.; Bai, J.; Plotto, A.; Dea, S. Electronic noses and tongues: Applications for the food and pharmaceutical industries. *Sensors* **2011**, *11*, 4744–4766. [[CrossRef](#)] [[PubMed](#)]
9. Sliwinska, M.; Wisniewska, P.; Dymerski, T.; Namiesnik, J.; Wardencki, W. Food analysis using artificial senses. *J. Agric. Food Chem.* **2014**, *62*, 1423–1448. [[CrossRef](#)] [[PubMed](#)]
10. He, X.J.; Hwang, H.M. Nanotechnology in food science: Functionality, applicability, and safety assessment. *J. Food Drug Anal.* **2016**, *24*, 671–681. [[CrossRef](#)] [[PubMed](#)]
11. Wilson, A. Diverse applications of electronic-nose technologies in agriculture and forestry. *Sensors* **2013**, *13*, 2295–2348. [[CrossRef](#)] [[PubMed](#)]
12. Baietto, M.; Wilson, A. Electronic-nose applications for fruit identification, ripeness and quality grading. *Sensors* **2015**, *15*, 899–931. [[CrossRef](#)] [[PubMed](#)]
13. Sekhon, B.S. Nanotechnology in agri-food production: An overview. *Nanotechnol. Sci. Appl.* **2014**, *7*, 31–53. [[CrossRef](#)] [[PubMed](#)]

14. Dasgupta, N.; Ranjan, S.; Mundekkad, D.; Ramalingam, C.; Shanker, R.; Kumar, A. Nanotechnology in agro-food: From field to plate. *Food Res. Int.* **2015**, *69*, 381–400. [[CrossRef](#)]
15. Parthibavarman, M.; Hariharan, V.; Sekar, C. High-sensitivity humidity sensor based on SnO₂ nanoparticles synthesized by microwave irradiation method. *Mater. Sci. Eng. C* **2011**, *31*, 840–844. [[CrossRef](#)]
16. Wang, Y.; Zhao, X.J.; Feng, Z.M.; Lu, G.Y.; Sun, T.; Xu, Y. Crystalline-phase-induced formation of fibre-intube TiO₂-SnO₂ fibres for a humidity sensor. *CrystEngComm* **2017**, *19*, 5528–5531. [[CrossRef](#)]
17. Hsu, C.L.; Su, I.L.; Hsueh, T.J. Tunable schottky contact humidity sensor based on S-doped ZnO nanowires on flexible pet substrate with piezotronic effect. *J. Alloys Compd.* **2017**, *705*, 722–733. [[CrossRef](#)]
18. Reig, C.S.; Lopez, A.D.; Ramos, M.H.; Ballester, V.A.C. Nanomaterials: A map for their selection in food packaging applications. *Packag. Technol. Sci.* **2014**, *27*, 839–866. [[CrossRef](#)]
19. Andrews, D.; Scholes, G.; Wiederrecht, G. *Comprehensive Nanoscience and Technology, Volume 1: Nanomaterials*; Elsevier Science Bv: Amsterdam, The Netherlands, 2011; pp. 1–635.
20. Galstyan, V.; Comini, E.; Faglia, G.; Sberveglieri, G. TiO₂ nanotubes: Recent advances in synthesis and gas sensing properties. *Sensors* **2013**, *13*, 14813–14838. [[CrossRef](#)] [[PubMed](#)]
21. Spencer, M.J.S. Gas sensing applications of 1d-nanostructured zinc oxide: Insights from density functional theory calculations. *Prog. Mater. Sci.* **2012**, *57*, 437–486. [[CrossRef](#)]
22. Galstyan, V.; Vomiero, A.; Comini, E.; Faglia, G.; Sberveglieri, G. TiO₂ nanotubular and nanoporous arrays by electrochemical anodization on different substrates. *RSC Adv.* **2011**, *1*, 1038–1044. [[CrossRef](#)]
23. Choi, M.J.; Cho, C.J.; Kim, K.C.; Pyeon, J.J.; Park, H.H.; Kim, H.S.; Han, J.H.; Kim, C.G.; Chung, T.M.; Park, T.J.; et al. SnO₂ thin films grown by atomic layer deposition using a novel sn precursor. *Appl. Surf. Sci.* **2014**, *320*, 188–194. [[CrossRef](#)]
24. Shaik, U.P.; Krishna, M.G. Single step formation of indium and tin doped ZnO nanowires by thermal oxidation of indium-zinc and tin-zinc metal films: Growth and optical properties. *Ceram. Int.* **2014**, *40*, 13611–13620. [[CrossRef](#)]
25. Li, W.; Li, Y.; Du, G.; Chen, N.; Liu, S.; Wang, S.; Huang, H.; Lu, C.; Niu, X. Enhanced electrical and optical properties of boron-doped ZnO films grown by low pressure chemical vapor deposition for amorphous silicon solar cells. *Ceram. Int.* **2016**, *42*, 1361–1365. [[CrossRef](#)]
26. Hu, P.; Han, N.; Zhang, D.; Ho, J.C.; Chen, Y. Highly formaldehyde-sensitive, transition-metal doped ZnO nanorods prepared by plasma-enhanced chemical vapor deposition. *Sens. Actuators B Chem.* **2012**, *169*, 74–80. [[CrossRef](#)]
27. Manuel, M.-M.; Ana, B.; Zineb, S.; Juan, P.E.; Angel, B.; Jose, C.; Gonzalez-Elipse, A.R. Vertical and tilted Ag-NPS@ZnO nanorods by plasma-enhanced chemical vapour deposition. *Nanotechnology* **2012**, *23*, 255303.
28. Haddad, K.; Abokifa, A.; Kavadiya, S.; Chadha, T.S.; Shetty, P.; Wang, Y.; Fortner, J.; Biswas, P. Growth of single crystal, oriented SnO₂ nanocolumn arrays by aerosol chemical vapour deposition. *CrystEngComm* **2016**, *18*, 7544–7553. [[CrossRef](#)]
29. Panigrahi, J.; Behera, D.; Mohanty, I.; Subudhi, U.; Nayak, B.B.; Acharya, B.S. Radio frequency plasma enhanced chemical vapor based ZnO thin film deposition on glass substrate: A novel approach towards antibacterial agent. *Appl. Surf. Sci.* **2011**, *258*, 304–311. [[CrossRef](#)]
30. Wang, J.; Dong, X.; Zhang, B.; Zhang, Y.; Wang, H.; Shi, Z.; Zhang, S.; Yin, W.; Du, G. P-type NiZnO thin films grown by photo-assist metal–organic chemical vapor deposition. *J. Alloys Compd.* **2013**, *579*, 160–164. [[CrossRef](#)]
31. Ye, Z.; Wang, T.; Wu, S.; Ji, X.; Zhang, Q. Na-doped ZnO nanorods fabricated by chemical vapor deposition and their optoelectrical properties. *J. Alloys Compd.* **2017**, *690*, 189–194. [[CrossRef](#)]
32. Comini, E.; Baratto, C.; Faglia, G.; Ferroni, M.; Vomiero, A.; Sberveglieri, G. Quasi-one dimensional metal oxide semiconductors: Preparation, characterization and application as chemical sensors. *Prog. Mater. Sci.* **2009**, *54*, 1–67. [[CrossRef](#)]
33. Zhang, Y.; Liu, M.; Ren, W.; Ye, Z.-G. Well-ordered ZnO nanotube arrays and networks grown by atomic layer deposition. *Appl. Surf. Sci.* **2015**, *340*, 120–125. [[CrossRef](#)]
34. Lim, Y.T.; Son, J.Y.; Rhee, J.S. Vertical ZnO nanorod array as an effective hydrogen gas sensor. *Ceram. Int.* **2013**, *39*, 887–890. [[CrossRef](#)]
35. Huang, Y.J.; Pandraud, G.; Sarro, P.M. The atomic layer deposition array defined by etch-back technique: A new method to fabricate TiO₂ nanopillars, nanotubes and nanochannel arrays. *Nanotechnology* **2012**, *23*, 485306. [[CrossRef](#)] [[PubMed](#)]

36. Lahiri, R.; Ghosh, A.; Dwivedi, S.M.M.D.; Chakrabartty, S.; Chinnamuthu, P.; Mondal, A. Performance of erbium-doped TiO₂ thin film grown by physical vapor deposition technique. *Appl. Phys. A* **2017**, *123*, 573. [[CrossRef](#)]
37. Comini, E.; Baratto, C.; Concina, I.; Faglia, G.; Falasconi, M.; Ferroni, M.; Galstyan, V.; Gobbi, E.; Ponzoni, A.; Vomiero, A.; et al. Metal oxide nanoscience and nanotechnology for chemical sensors. *Sens. Actuators B Chem.* **2013**, *179*, 3–20. [[CrossRef](#)]
38. George, A.; Kumari, P.; Sooin, N.; Roy, S.S.; McLaughlin, J.A. Microstructure and field emission characteristics of ZnO nanoneedles grown by physical vapor deposition. *Mater. Chem. Phys.* **2010**, *123*, 634–638. [[CrossRef](#)]
39. Dlugosch, T.; Chnani, A.; Muralidhar, P.; Schirmer, A.; Biskupek, J.; Strehle, S. Thermal oxidation synthesis of crystalline iron-oxide nanowires on low-cost steel substrates for solar water splitting. *Semicond. Sci. Technol.* **2017**, *32*, 084001. [[CrossRef](#)]
40. Kim, D.; Leem, J.Y. Catalyst-free synthesis of ZnO nanorods by thermal oxidation of Zn films at various temperatures and their characterization. *J. Nanosci. Nanotechnol.* **2017**, *17*, 5826–5829. [[CrossRef](#)]
41. Comini, E.; Galstyan, V.; Faglia, G.; Bontempi, E.; Sberveglieri, G. Highly conductive titanium oxide nanotubes chemical sensors. *Microporous Mesoporous Mater.* **2015**, *208*, 165–170. [[CrossRef](#)]
42. Ellis, B.L.; Knauth, P.; Djenizian, T. Three-dimensional self-supported metal oxides for advanced energy storage. *Adv. Mater.* **2014**, *26*, 3368–3397. [[CrossRef](#)] [[PubMed](#)]
43. Galstyan, V.; Comini, E.; Faglia, G.; Sberveglieri, G. Synthesis of self-ordered and well-aligned Nb₂O₅ nanotubes. *CrystEngComm* **2014**, *16*, 10273–10279. [[CrossRef](#)]
44. Galstyan, V.; Vomiero, A.; Concina, I.; Braga, A.; Brisotto, M.; Bontempi, E.; Faglia, G.; Sberveglieri, G. Vertically aligned TiO₂ nanotubes on plastic substrates for flexible solar cells. *Small* **2011**, *7*, 2437–2442. [[CrossRef](#)] [[PubMed](#)]
45. Galstyan, V.; Comini, E.; Baratto, C.; Faglia, G.; Sberveglieri, G. Nanostructured ZnO chemical gas sensors. *Ceram. Int.* **2015**, *41*, 14239–14244. [[CrossRef](#)]
46. Rana, A.u.H.S.; Chang, S.-B.; Chae, H.U.; Kim, H.-S. Structural, optical, electrical and morphological properties of different concentration sol-gel ZnO seeds and consanguineous ZnO nanostructured growth dependence on seeds. *J. Alloys Compd.* **2017**, *729*, 571–582. [[CrossRef](#)]
47. Valerio, L.R.; Mamani, N.C.; de Zevallos, A.O.; Mesquita, A.; Bernardi, M.I.B.; Doriguetto, A.C.; de Carvalho, H.B. Preparation and structural-optical characterization of dip-coated nanostructured co-doped ZnO dilute magnetic oxide thin films. *Rsc Adv.* **2017**, *7*, 20611–20619. [[CrossRef](#)]
48. Richard, D.; Romero, M.; Faccio, R. Experimental and theoretical study on the structural, electrical and optical properties of tantalum-doped ZnO nanoparticles prepared via sol-gel acetate route. *Ceram. Int.* **2018**, *44*, 703–711. [[CrossRef](#)]
49. Zhang, Z.; Yin, C.; Yang, L.; Jia, W.; Zhou, J.; Xu, H.; Cao, D. H₂ response characteristics for sol-gel-derived WO₃-SnO₂ dual-layer thin films. *Ceram. Int.* **2017**, *43*, 6693–6699. [[CrossRef](#)]
50. Yao, S.; Qu, F.; Wang, G.; Wu, X. Facile hydrothermal synthesis of WO₃ nanorods for photocatalysts and supercapacitors. *J. Alloys Compd.* **2017**, *724*, 695–702. [[CrossRef](#)]
51. Cao, S.; Zhao, C.; Han, T.; Peng, L. Hydrothermal synthesis, characterization and gas sensing properties of the WO₃ nanofibers. *Mater. Lett.* **2016**, *169*, 17–20. [[CrossRef](#)]
52. Yu, Z.; Qu, X.; Yang, W.; Peng, J.; Xu, Z. A facile hydrothermal synthesis and memristive switching performance of rutile TiO₂ nanowire arrays. *J. Alloys Compd.* **2016**, *688*, 37–43. [[CrossRef](#)]
53. Yin, M.; Yao, Y.; Fan, H.; Liu, S. WO₃-SnO₂ nanosheet composites: Hydrothermal synthesis and gas sensing mechanism. *J. Alloys Compd.* **2018**, *736*, 322–331. [[CrossRef](#)]
54. Sun, K.C.; Qadir, M.B.; Jeong, S.H. Hydrothermal synthesis of TiO₂ nanotubes and their application as an over-layer for dye-sensitized solar cells. *RSC Adv.* **2014**, *4*, 23223–23230. [[CrossRef](#)]
55. Perillo, P.M.; Rodríguez, D.F. Low temperature trimethylamine flexible gas sensor based on TiO₂ membrane nanotubes. *J. Alloys Compd.* **2016**, *657*, 765–769. [[CrossRef](#)]
56. Liu, L.; Song, P.; Yang, Z.; Wang, Q. Highly sensitive and selective trimethylamine sensors based on WO₃ nanorods decorated with Au nanoparticles. *Phys. E Low-Dimens. Syst. Nanostruct.* **2017**, *90*, 109–115. [[CrossRef](#)]
57. Chu, X.; Zhou, S.; Dong, Y.; Sun, W.; Ge, X. Trimethylamine gas sensor based on Cr³⁺ doped ZnO nanorods/nanoparticles prepared via solvothermal method. *Mater. Chem. Phys.* **2011**, *131*, 27–31. [[CrossRef](#)]
58. Meng, F.; Zheng, H.; Sun, Y.; Li, M.; Liu, J. Trimethylamine sensors based on Au-modified hierarchical porous single-crystalline ZnO nanosheets. *Sensors* **2017**, *17*, 1478. [[CrossRef](#)] [[PubMed](#)]

59. Zhang, J.; Song, P.; Li, Z.; Zhang, S.; Yang, Z.; Wang, Q. Enhanced trimethylamine sensing performance of single-crystal MoO₃ nanobelts decorated with Au nanoparticles. *J. Alloys Compd.* **2016**, *685*, 1024–1033. [[CrossRef](#)]
60. Woo, H.-S.; Na, C.; Kim, I.-D.; Lee, J.-H. Highly sensitive and selective trimethylamine sensor using one-dimensional ZnO-Cr₂O₃ hetero-nanostructures. *Nanotechnology* **2012**, *23*, 245501. [[CrossRef](#)] [[PubMed](#)]
61. Lee, C.-S.; Kim, I.-D.; Lee, J.-H. Selective and sensitive detection of trimethylamine using ZnO-In₂O₃ composite nanofibers. *Sens. Actuators B Chem.* **2013**, *181*, 463–470. [[CrossRef](#)]
62. Kwak, C.-H.; Woo, H.-S.; Lee, J.-H. Selective trimethylamine sensors using Cr₂O₃-decorated SnO₂ nanowires. *Sens. Actuators B Chem.* **2014**, *204*, 231–238. [[CrossRef](#)]
63. Lou, Z.; Li, F.; Deng, J.; Wang, L.; Zhang, T. Branch-like hierarchical heterostructure (α -Fe₂O₃/TiO₂): A novel sensing material for trimethylamine gas sensor. *ACS Appl. Mater. Interfaces* **2013**, *5*, 12310–12316. [[CrossRef](#)] [[PubMed](#)]
64. Chun, H.-N.; Kim, B.; Shin, H.-S. Evaluation of a freshness indicator for quality of fish products during storage. *Food Sci. Biotechnol.* **2014**, *23*, 1719–1725. [[CrossRef](#)]
65. Du, J.; Wang, H.; Zhao, R.; Xie, Y.; Yao, H. Surfactant-assisted synthesis of the pencil-like zinc oxide and its sensing properties. *Mater. Lett.* **2013**, *107*, 259–261. [[CrossRef](#)]
66. Zhang, L.; Zhao, J.; Lu, H.; Li, L.; Zheng, J.; Zhang, J.; Li, H.; Zhu, Z. Highly sensitive and selective dimethylamine sensors based on hierarchical ZnO architectures composed of nanorods and nanosheet-assembled microspheres. *Sens. Actuators B Chem.* **2012**, *171*, 1101–1109. [[CrossRef](#)]
67. Wojnowski, W.; Majchrzak, T.; Dymerski, T.; Gębicki, J.; Namieśnik, J. Portable electronic nose based on electrochemical sensors for food quality assessment. *Sensors* **2017**, *17*, 2715. [[CrossRef](#)] [[PubMed](#)]
68. Li, Y.; Ban, H.; Yang, M. Highly sensitive NH₃ gas sensors based on novel polypyrrole-coated SnO₂ nanosheet nanocomposites. *Sens. Actuators B Chem.* **2016**, *224*, 449–457. [[CrossRef](#)]
69. Jain, S.; Karmakar, N.; Shah, A.; Kothari, D.C.; Mishra, S.; Shimpi, N.G. Ammonia detection of 1-d ZnO/polypyrrole nanocomposite: Effect of CSA doping and their structural, chemical, thermal and gas sensing behavior. *Appl. Surf. Sci.* **2017**, *396*, 1317–1325. [[CrossRef](#)]
70. Tai, H.; Jiang, Y.; Xie, G.; Yu, J.; Chen, X.; Ying, Z. Influence of polymerization temperature on NH₃ response of PANI/TiO₂ thin film gas sensor. *Sens. Actuators B Chem.* **2008**, *129*, 319–326. [[CrossRef](#)]
71. Das, M.; Sarkar, D. One-pot synthesis of zinc oxide-polyaniline nanocomposite for fabrication of efficient room temperature ammonia gas sensor. *Ceram. Int.* **2017**, *43*, 11123–11131. [[CrossRef](#)]
72. Shingange, K.; Tshabalala, Z.P.; Ntwaeaborwa, O.M.; Motaung, D.E.; Mhlongo, G.H. Highly selective NH₃ gas sensor based on Au loaded ZnO nanostructures prepared using microwave-assisted method. *J. Colloid Interface Sci.* **2016**, *479*, 127–138. [[CrossRef](#)] [[PubMed](#)]
73. Li, R.; Jiang, K.; Chen, S.; Lou, Z.; Huang, T.; Chen, D.; Shen, G. SnO₂/SnS₂ nanotubes for flexible room-temperature NH₃ gas sensors. *RSC Adv.* **2017**, *7*, 52503–52509. [[CrossRef](#)]
74. Warren, M.W.; Larick, D.K.; Ball, H.R. Volatiles and sensory characteristics of cooked egg-yolk, white and their combinations. *J. Food Sci.* **1995**, *60*, 79–84. [[CrossRef](#)]
75. Perillo, P.; Rodríguez, D. TiO₂ nanotubes membrane flexible sensor for low-temperature H₂S detection. *Chemosensors* **2016**, *4*, 15. [[CrossRef](#)]
76. Yu, T.; Cheng, X.; Zhang, X.; Sui, L.; Xu, Y.; Gao, S.; Zhao, H.; Huo, L. Highly sensitive H₂S detection sensors at low temperature based on hierarchically structured NiO porous nanowall arrays. *J. Mater. Chem. A* **2015**, *3*, 11991–11999. [[CrossRef](#)]
77. Li, Z.; Wang, N.; Lin, Z.; Wang, J.; Liu, W.; Sun, K.; Fu, Y.Q.; Wang, Z. Room-temperature high-performance H₂S sensor based on porous CuO nanosheets prepared by hydrothermal method. *ACS Appl. Mater. Interfaces* **2016**, *8*, 20962–20968. [[CrossRef](#)] [[PubMed](#)]
78. Yeh, B.-Y.; Jian, B.-S.; Wang, G.-J.; Tseng, W.J. CuO/V₂O₅ hybrid nanowires for highly sensitive and selective H₂S gas sensor. *RSC Adv.* **2017**, *7*, 49605–49612. [[CrossRef](#)]
79. Jiang, P.; Zhang, H.; Chen, C.; Liang, J.; Luo, Y.; Zhang, M.; Cai, M. Co₃O₄-SnO₂ nanobox sensor with a pn junction and semiconductor-conductor transformation for high selectivity and sensitivity detection of H₂S. *CrystEngComm* **2017**, *19*, 5742–5748. [[CrossRef](#)]
80. Guo, W.; Mei, L.; Wen, J.; Ma, J. High-response H₂S sensor based on ZnO/SnO₂ heterogeneous nanospheres. *RSC Adv.* **2016**, *6*, 15048–15053. [[CrossRef](#)]

81. Yoon, J.-W.; Hong, Y.J.; Chan Kang, Y.; Lee, J.-H. High performance chemiresistive H₂S sensors using Ag-loaded SnO₂ yolk-shell nanostructures. *RSC Adv.* **2014**, *4*, 16067–16074. [[CrossRef](#)]
82. Yang, T.; Yang, Q.; Xiao, Y.; Sun, P.; Wang, Z.; Gao, Y.; Ma, J.; Sun, Y.; Lu, G. A pulse-driven sensor based on ordered mesoporous Ag₂O/SnO₂ with improved H₂S-sensing performance. *Sens. Actuators B Chem.* **2016**, *228*, 529–538. [[CrossRef](#)]
83. Kheel, H.; Sun, G.-J.; Lee, J.K.; Lee, S.; Dwivedi, R.P.; Lee, C. Enhanced H₂S sensing performance of TiO₂-decorated α -Fe₂O₃ nanorod sensors. *Ceram. Int.* **2016**, *42*, 18597–18604. [[CrossRef](#)]
84. Wang, Y.; Liu, B.; Xiao, S.; Wang, X.; Sun, L.; Li, H.; Xie, W.; Li, Q.; Zhang, Q.; Wang, T. Low-temperature H₂S detection with hierarchical Cr-doped WO₃ microspheres. *ACS Appl. Mater. Interfaces* **2016**, *8*, 9674–9683. [[CrossRef](#)] [[PubMed](#)]
85. Tong, X.; Shen, W.; Chen, X.; Corriou, J.-P. A fast response and recovery H₂S gas sensor based on free-standing TiO₂ nanotube array films prepared by one-step anodization method. *Ceram. Int.* **2017**, *43*, 14200–14209. [[CrossRef](#)]
86. Hosseini, Z.S.; Mortezaali, A.; Irajizad, A.; Fardindoost, S. Sensitive and selective room temperature H₂S gas sensor based on Au sensitized vertical ZnO nanorods with flower-like structures. *J. Alloys Compd.* **2015**, *628*, 222–229. [[CrossRef](#)]
87. Nimbalkar, A.R.; Patil, M.G. Synthesis of highly selective and sensitive Cu-doped ZnO thin film sensor for detection of H₂S gas. *Mater. Sci. Semicond. Process.* **2017**, *71*, 332–341. [[CrossRef](#)]
88. Hyun, S.K.; Sun, G.-J.; Lee, J.K.; Lee, C.; In Lee, W.; Kim, H.W. Ethanol gas sensing using a networked pbo-decorated SnO₂ nanowires. *Thin Solid Films* **2017**, *637*, 21–26. [[CrossRef](#)]
89. Galstyan, V.; Comini, E.; Baratto, C.; Ponzoni, A.; Ferroni, M.; Poli, N.; Bontempi, E.; Brisotto, M.; Faglia, G.; Sberveglieri, G. Large surface area biphasic titania for chemical sensing. *Sens. Actuators B Chem.* **2015**, *209*, 1091–1096. [[CrossRef](#)]
90. Choi, S.; Bonyani, M.; Sun, G.-J.; Lee, J.K.; Hyun, S.K.; Lee, C. Cr₂O₃ nanoparticle-functionalized WO₃ nanorods for ethanol gas sensors. *Appl. Surf. Sci.* **2018**, *432*, 241–249. [[CrossRef](#)]
91. Tan, J.; Dun, M.; Li, L.; Zhao, J.; Tan, W.; Lin, Z.; Huang, X. Synthesis of hollow and hollowed-out Co₃O₄ microspheres assembled by porous ultrathin nanosheets for ethanol gas sensors: Responding and recovering in one second. *Sens. Actuators B Chem.* **2017**, *249*, 44–52. [[CrossRef](#)]
92. Ben Amor, M.; Boukhachem, A.; Labidi, A.; Boubaker, K.; Amlouk, M. Physical investigations on Cd doped NiO thin films along with ethanol sensing at relatively low temperature. *J. Alloys Compd.* **2017**, *693*, 490–499. [[CrossRef](#)]
93. Jeong, Y.J.; Koo, W.-T.; Jang, J.-S.; Kim, D.-H.; Kim, M.-H.; Kim, I.-D. Nanoscale PtO₂ catalysts-loaded SnO₂ multichannel nanofibers toward highly sensitive acetone sensor. *ACS Appl. Mater. Interfaces* **2018**, *10*, 2016–2025. [[CrossRef](#)] [[PubMed](#)]
94. Shen, J.-Y.; Wang, M.-D.; Wang, Y.-F.; Hu, J.-Y.; Zhu, Y.; Zhang, Y.X.; Li, Z.-J.; Yao, H.-C. Iron and carbon codoped WO₃ with hierarchical walnut-like microstructure for highly sensitive and selective acetone sensor. *Sens. Actuators B Chem.* **2018**, *256*, 27–37. [[CrossRef](#)]
95. Wang, C.; Liu, J.; Yang, Q.; Sun, P.; Gao, Y.; Liu, F.; Zheng, J.; Lu, G. Ultrasensitive and low detection limit of acetone gas sensor based on W-doped NiO hierarchical nanostructure. *Sens. Actuators B Chem.* **2015**, *220*, 59–67. [[CrossRef](#)]
96. Mishra, R.K.; Murali, G.; Kim, T.-H.; Kim, J.H.; Lim, Y.J.; Kim, B.-S.; Sahay, P.P.; Lee, S.H. Nanocube In₂O₃@RGO heterostructure based gas sensor for acetone and formaldehyde detection. *RSC Adv.* **2017**, *7*, 38714–38724. [[CrossRef](#)]
97. Konduru, T.; Rains, G.; Li, C. A customized metal oxide semiconductor-based gas sensor array for onion quality evaluation: System development and characterization. *Sensors* **2015**, *15*, 1252–1273. [[CrossRef](#)] [[PubMed](#)]
98. Russo, M.; Serra, D.; Suraci, F.; Di Sanzo, R.; Fuda, S.; Postorino, S. The potential of e-nose aroma profiling for identifying the geographical origin of licorice (*Glycyrrhiza glabra* L.) roots. *Food Chem.* **2014**, *165*, 467–474. [[CrossRef](#)] [[PubMed](#)]
99. Pacioni, G.; Cerretani, L.; Procida, G.; Cichelli, A. Composition of commercial truffle flavored oils with GC–MS analysis and discrimination with an electronic nose. *Food Chem.* **2014**, *146*, 30–35. [[CrossRef](#)] [[PubMed](#)]
100. Zhang, J.; Liu, X.H.; Neri, G.; Pinna, N. Nanostructured materials for room-temperature gas sensors. *Adv. Mater.* **2016**, *28*, 795–831. [[CrossRef](#)] [[PubMed](#)]

101. Joshi, N.; Hayasaka, T.; Liu, Y.; Liu, H.; Oliveira, O.N.; Lin, L. A review on chemiresistive room temperature gas sensors based on metal oxide nanostructures, graphene and 2D transition metal dichalcogenides. *Microchim. Acta* **2018**, *185*, 213. [[CrossRef](#)] [[PubMed](#)]
102. Liu, X.; Ma, T.; Pinna, N.; Zhang, J. Two-dimensional nanostructured materials for gas sensing. *Adv. Funct. Mater.* **2017**, *27*, 1702168. [[CrossRef](#)]
103. Barsan, N.; Schweizer-Berberich, M.; Gopel, W. Fundamental and practical aspects in the design of nanoscaled SnO₂ gas sensors: A status report. *Fresenius J. Anal. Chem.* **1999**, *365*, 287–304. [[CrossRef](#)]
104. Lelono, D.; Triyana, K.; Hartati, S.; Istiyanto, J.E. Classification of indonesia black teas based on quality by using electronic nose and principal component analysis. In *Advances of Science and Technology for Society*; Nuringtyas, T.R., Roto, R., Widyaparaga, A., Mahardika, M., Kusumaadmaja, A., Sholihun, Hadi, N., Eds.; AIP: College Park, MD, USA, 2016; Volume 1755.
105. Severini, C.; Derossi, A.; Fiore, A.G.; Ricci, I.; Marone, M. The electronic nose system: Study on the global aromatic profile of espresso coffee prepared with two types of coffee filter holders. *Eur. Food Res. Technol.* **2016**, *242*, 2083–2091. [[CrossRef](#)]
106. Gobbi, E.; Falasconi, M.; Zambotti, G.; Sberveglieri, V.; Pulvirenti, A.; Sberveglieri, G. Rapid diagnosis of enterobacteriaceae in vegetable soups by a metal oxide sensor based electronic nose. *Sens. Actuators B Chem.* **2015**, *207*, 1104–1113. [[CrossRef](#)]
107. Ghosh, A.; Ray, H.; Ghosh, T.K.; Das, A.; Bhattacharyya, N. Generic handheld e-nose platform for quality assessment of agricultural produces and biomedical applications. In *Proceedings of the Nose2014: 4th International Conference on Environmental Odour Monitoring and Control*, Venice, Italy, 14–17 September 2014; Volume 40, pp. 259–264.
108. Sanaeifar, A.; Mohtasebi, S.S.; Ghasemi-Varnamkhasti, M.; Ahmadi, H. Application of mos based electronic nose for the prediction of banana quality properties. *Measurement* **2016**, *82*, 105–114. [[CrossRef](#)]
109. Trirongjitmoah, S.; Juengmunkong, Z.; Srikulnath, K.; Somboon, P. Classification of garlic cultivars using an electronic nose. *Comput. Electron. Agric.* **2015**, *113*, 148–153. [[CrossRef](#)]
110. Qiu, S.; Wang, J.; Gao, L. Qualification and quantisation of processed strawberry juice based on electronic nose and tongue. *LWT-Food Sci. Technol.* **2015**, *60*, 115–123. [[CrossRef](#)]
111. Güney, S.; Atasoy, A. Study of fish species discrimination via electronic nose. *Comput. Electron. Agric.* **2015**, *119*, 83–91. [[CrossRef](#)]
112. Severini, C.; Ricci, I.; Marone, M.; Derossi, A.; De Pilli, T. Changes in the aromatic profile of espresso coffee as a function of the grinding grade and extraction time: A study by the electronic nose system. *J. Agric. Food Chem.* **2015**, *63*, 2321–2327. [[CrossRef](#)] [[PubMed](#)]
113. Hasan, N.; Ejaz, N.; Ejaz, W.; Kim, H. Meat and fish freshness inspection system based on odor sensing. *Sensors* **2012**, *12*, 15542–15557. [[CrossRef](#)] [[PubMed](#)]
114. Xu, M.; Ye, L.; Wang, J.; Wei, Z.; Cheng, S. Quality tracing of peanuts using an array of metal-oxide based gas sensors combined with chemometrics methods. *Postharvest Biol. Technol.* **2017**, *128*, 98–104. [[CrossRef](#)]
115. Xu, L.; Yu, X.; Liu, L.; Zhang, R. A novel method for qualitative analysis of edible oil oxidation using an electronic nose. *Food Chem.* **2016**, *202*, 229–235. [[CrossRef](#)] [[PubMed](#)]
116. Tian, X.-Y.; Cai, Q.; Zhang, Y.-M. Rapid classification of hairtail fish and pork freshness using an electronic nose based on the PCA method. *Sensors* **2012**, *12*, 260–277. [[CrossRef](#)] [[PubMed](#)]
117. Dymerski, T.; Gebicki, J.; Wardencki, W.; Namiesnik, J. Application of an electronic nose instrument to fast classification of polish honey types. *Sensors* **2014**, *14*, 10709–10724. [[CrossRef](#)] [[PubMed](#)]
118. Yemmireddy, V.K.; Hung, Y.-C. Effect of binder on the physical stability and bactericidal property of titanium dioxide (TiO₂) nanocoatings on food contact surfaces. *Food Control* **2015**, *57*, 82–88. [[CrossRef](#)]
119. Mofokeng, J.P.; Luyt, A.S. Morphology and thermal degradation studies of melt-mixed poly(hydroxybutyrate-co-valerate) (PHBV)/poly(ϵ -caprolactone) (PCL) biodegradable polymer blend nanocomposites with TiO₂ as filler. *J. Mater. Sci.* **2015**, *50*, 3812–3824. [[CrossRef](#)]
120. Lin, Q.B.; Li, H.; Zhong, H.N.; Zhao, Q.; Xiao, D.H.; Wang, Z.W. Migration of ti from nano-TiO₂-polyethylene composite packaging into food simulants. *Food Addit. Contam. Part A-Chem. Anal. Control Expos. Risk Assess.* **2014**, *31*, 1284–1290. [[CrossRef](#)] [[PubMed](#)]
121. Yemmireddy, V.K.; Farrell, G.D.; Hung, Y.C. Development of titanium dioxide (TiO₂) nanocoatings on food contact surfaces and method to evaluate their durability and photocatalytic bactericidal property. *J. Food Sci.* **2015**, *80*, N1903–N1911. [[CrossRef](#)] [[PubMed](#)]

122. Pathakoti, K.; Morrow, S.; Han, C.; Pelaez, M.; He, X.; Dionysiou, D.D.; Hwang, H.-M. Photoinactivation of escherichia coli by sulfur-doped and nitrogen–fluorine-codoped TiO₂ nanoparticles under solar simulated light and visible light irradiation. *Environ. Sci. Technol.* **2013**, *47*, 9988–9996. [[CrossRef](#)] [[PubMed](#)]
123. Kubacka, A.; Diez, M.S.; Rojo, D.; Bargiela, R.; Ciordia, S.; Zapico, I.; Albar, J.P.; Barbas, C.; dos Santos, V.; Fernandez-Garcia, M.; et al. Understanding the antimicrobial mechanism of TiO₂-based nanocomposite films in a pathogenic bacterium. *Sci. Rep.* **2014**, *4*, 4134. [[CrossRef](#)] [[PubMed](#)]
124. Farhoodi, M. Nanocomposite materials for food packaging applications: Characterization and safety evaluation. *Food Eng. Rev.* **2016**, *8*, 35–51. [[CrossRef](#)]
125. Youssef, A.M.; El-Sayed, S.M.; Salama, H.H.; El-Sayed, H.S.; Dufresne, A. Evaluation of bionanocomposites as packaging material on properties of soft white cheese during storage period. *Carbohydr. Polym.* **2015**, *132*, 274–285. [[CrossRef](#)] [[PubMed](#)]
126. Youssef, A.M.; El-Sayed, S.M.; El-Sayed, H.S.; Salama, H.H.; Dufresne, A. Enhancement of egyptian soft white cheese shelf life using a novel chitosan/carboxymethyl cellulose/zinc oxide bionanocomposite film. *Carbohydr. Polym.* **2016**, *151*, 9–19. [[CrossRef](#)] [[PubMed](#)]
127. Krehula, L.K.; Papić, A.; Krehula, S.; Gilja, V.; Foglar, L.; Hrnjak-Murgić, Z. Properties of uv protective films of poly(vinyl-chloride)/TiO₂ nanocomposites for food packaging. *Polym. Bull.* **2017**, *74*, 1387–1404. [[CrossRef](#)]
128. He, Q.Y.; Huang, Y.; Lin, B.B.; Wang, S.Y. A nanocomposite film fabricated with simultaneously extracted protein-polysaccharide from a marine alga and TiO₂ nanoparticles. *J. Appl. Phycol.* **2017**, *29*, 1541–1552. [[CrossRef](#)]
129. Goudarzi, V.; Shahabi-Ghahfarrokhi, I.; Babaei-Ghazvini, A. Preparation of ecofriendly uv-protective food packaging material by starch/TiO₂ bio-nanocomposite: Characterization. *Int. J. Biol. Macromol.* **2017**, *95*, 306–313. [[CrossRef](#)] [[PubMed](#)]
130. Luo, Z.S.; Qin, Y.; Ye, Q.Y. Effect of nano-TiO₂-ldpe packaging on microbiological and physicochemical quality of pacific white shrimp during chilled storage. *Int. J. Food Sci. Technol.* **2015**, *50*, 1567–1573. [[CrossRef](#)]
131. Bodaghi, H.; Mostofi, Y.; Oromiehie, A.; Zamani, Z.; Ghanbarzadeh, B.; Costa, C.; Conte, A.; Del Nobile, M.A. Evaluation of the photocatalytic antimicrobial effects of a TiO₂ nanocomposite food packaging film by in vitro and in vivo tests. *LWT-Food Sci. Technol.* **2013**, *50*, 702–706. [[CrossRef](#)]
132. Bodaghi, H.; Mostofi, Y.; Oromiehie, A.; Ghanbarzadeh, B.; Hagh, Z.G. Synthesis of clay-TiO₂ nanocomposite thin films with barrier and photocatalytic properties for food packaging application. *J. Appl. Polym. Sci.* **2015**, *132*. [[CrossRef](#)]
133. De Chiara, M.L.V.; Pal, S.; Licciulli, A.; Amodio, M.L.; Colelli, G. Photocatalytic degradation of ethylene on mesoporous TiO₂/SiO₂ nanocomposites: Effects on the ripening of mature green tomatoes. *Biosyst. Eng.* **2015**, *132*, 61–70. [[CrossRef](#)]
134. Kaewklin, P.; Siripatrawan, U.; Suwanagul, A.; Lee, Y.S. Active packaging from chitosan-titanium dioxide nanocomposite film for prolonging storage life of tomato fruit. *Int. J. Biol. Macromol.* **2018**, *112*, 523–529. [[CrossRef](#)] [[PubMed](#)]
135. Alizadeh Sani, M.; Ehsani, A.; Hashemi, M. Whey protein isolate/cellulose nanofibre/TiO₂ nanoparticle/rosemary essential oil nanocomposite film: Its effect on microbial and sensory quality of lamb meat and growth of common foodborne pathogenic bacteria during refrigeration. *Int. J. Food Microbiol.* **2017**, *251*, 8–14. [[CrossRef](#)] [[PubMed](#)]
136. Jin, B.; Li, X.; Zhou, X.; Xu, X.; Jian, H.; Li, M.; Guo, K.; Guan, J.; Yan, S. Fabrication and characterization of nanocomposite film made from a jackfruit filum polysaccharide incorporating TiO₂ nanoparticles by photocatalysis. *RSC Adv.* **2017**, *7*, 16931–16937. [[CrossRef](#)]
137. Naik, K.; Kowshik, M. Anti-quorum sensing activity of AgCl-TiO₂ nanoparticles with potential use as active food packaging material. *J. Appl. Microbiol.* **2014**, *117*, 972–983. [[CrossRef](#)] [[PubMed](#)]
138. Peter, A.; Tegla, D.; Giurgiulescu, L.; Cozmuta, A.M.; Nicula, C.; Cozmuta, L.M.; Vagelas, I. Development of Ag/TiO₂-SiO₂-coated food packaging film and its role in preservation of green lettuce during storage. *Carpathian J. Food Sci. Technol.* **2015**, *7*, 88–96.
139. Cozmuta, A.M.; Peter, A.; Cozmuta, L.M.; Nicula, C.; Crisan, L.; Baia, L.; Turila, A. Active packaging system based on Ag/TiO₂ nanocomposite used for extending the shelf life of bread. Chemical and microbiological investigations. *Packag. Technol. Sci.* **2015**, *28*, 271–284. [[CrossRef](#)]

140. Peter, A.; Mihaly-Cozmuta, L.; Mihaly-Cozmuta, A.; Nicula, C.; Ziemkowska, W.; Basiak, D.; Danciu, V.; Vulpoi, A.; Baia, L.; Falup, A.; et al. Changes in the microbiological and chemical characteristics of white bread during storage in paper packages modified with Ag/TiO₂-SiO₂, Ag/N-TiO₂ or Au/TiO₂. *Food Chem.* **2016**, *197*, 790–798. [[CrossRef](#)] [[PubMed](#)]
141. Li, W.H.; Li, L.; Zhang, H.; Yuan, M.L.; Qin, Y.Y. Evaluation of pla nanocomposite films on physicochemical and microbiological properties of refrigerated cottage cheese. *J. Food Process. Preserv.* **2018**, *42*. [[CrossRef](#)]
142. Oleyaei, S.A.; Zahedi, Y.; Ghanbarzadeh, B.; Moayedi, A.A. Modification of physicochemical and thermal properties of starch films by incorporation of TiO₂ nanoparticles. *Int. J. Biol. Macromol.* **2016**, *89*, 256–264. [[CrossRef](#)] [[PubMed](#)]
143. Shaili, T.; Abdorreza, M.N.; Fariborz, N. Functional, thermal, and antimicrobial properties of soluble soybean polysaccharide biocomposites reinforced by nano TiO₂. *Carbohydr. Polym.* **2015**, *134*, 726–731. [[CrossRef](#)] [[PubMed](#)]
144. Vejdani, A.; Ojagh, S.M.; Adeli, A.; Abdollahi, M. Effect of TiO₂ nanoparticles on the physico-mechanical and ultraviolet light barrier properties of fish gelatin/agar bilayer film. *LWT-Food Sci. Technol.* **2016**, *71*, 88–95. [[CrossRef](#)]
145. El-Wakil, N.A.; Hassan, E.A.; Abou-Zeid, R.E.; Dufresne, A. Development of wheat gluten/nanocellulose/titanium dioxide nanocomposites for active food packaging. *Carbohydr. Polym.* **2015**, *124*, 337–346. [[CrossRef](#)] [[PubMed](#)]
146. Othman, S.H.; Abd Salam, N.R.; Zainal, N.; Basha, R.K.; Talib, R.A. Antimicrobial activity of TiO₂ nanoparticle-coated film for potential food packaging applications. *Int. J. Photoenergy* **2014**. [[CrossRef](#)]
147. Zhang, X.D.; Xiao, G.; Wang, Y.Q.; Zhao, Y.; Su, H.J.; Tan, T.W. Preparation of chitosan-TiO₂ composite film with efficient antimicrobial activities under visible light for food packaging applications. *Carbohydr. Polym.* **2017**, *169*, 101–107. [[CrossRef](#)] [[PubMed](#)]
148. Gupta, K.; Singh, R.P.; Pandey, A.; Pandey, A. Photocatalytic antibacterial performance of TiO₂ and Ag-doped TiO₂ against *S. aureus*, *P. aeruginosa* and *E. coli*. *Beilstein J. Nanotechnol.* **2013**, *4*, 345–351. [[CrossRef](#)] [[PubMed](#)]
149. Venkatasubbu, G.D.; Baskar, R.; Anusuya, T.; Seshan, C.A.; Chelliah, R. Toxicity mechanism of titanium dioxide and zinc oxide nanoparticles against food pathogens. *Colloids Surf. B Biointerfaces* **2016**, *148*, 600–606. [[CrossRef](#)] [[PubMed](#)]
150. Marcous, A.; Rasouli, S.; Ardestani, F. Low-density polyethylene films loaded by titanium dioxide and zinc oxide nanoparticles as a new active packaging system against escherichia coli O157:H7 in fresh calf minced meat. *Packag. Technol. Sci.* **2017**, *30*, 693–701. [[CrossRef](#)]
151. Noshirvani, N.; Ghanbarzadeh, B.; Mokarram, R.R.; Hashemi, M.; Coma, V. Preparation and characterization of active emulsified films based on chitosan-carboxymethyl cellulose containing zinc oxide nano particles. *Int. J. Biol. Macromol.* **2017**, *99*, 530–538. [[CrossRef](#)] [[PubMed](#)]
152. Noshirvani, N.; Ghanbarzadeh, B.; Rezaei Mokarram, R.; Hashemi, M. Novel active packaging based on carboxymethyl cellulose-chitosan-ZnO nps nanocomposite for increasing the shelf life of bread. *Food Packag. Shelf Life* **2017**, *11*, 106–114. [[CrossRef](#)]
153. Rescek, A.; Krehula, L.K.; Katancic, Z.; Hrnjak-Murgic, Z. Active bilayer pe/pcl films for food packaging modified with zinc oxide and casein. *Croat. Chem. Acta* **2015**, *88*, 461–473. [[CrossRef](#)]
154. Al-Naamani, L.; Dobretsov, S.; Dutta, J. Chitosan-zinc oxide nanoparticle composite coating for active food packaging applications. *Innov. Food Sci. Emerg. Technol.* **2016**, *38*, 231–237. [[CrossRef](#)]
155. Threepopnatkul, P.; Wongnarat, C.; Intolo, W.; Suato, S.; Kulsetthanchalee, C. Effect of TiO₂ and ZnO on thin film properties of pet/pbs blend for food packaging applications. *Energy Procedia* **2014**, *56*, 102–111. [[CrossRef](#)]

